Stem Cell Reports
Article
OPEN ACCESS

CD13 and ROR2 Permit Isolation of Highly Enriched Cardiac Mesoderm from Differentiating Human Embryonic Stem Cells

Rhys J.P. Skelton,[1,2,3] Bevin Brady,[4] Suhail Khoja,[1,2] Debashis Sahoo,[4] James Engel,[1,2] Deevina Arasaratnam,[3] Kholoud K. Saleh,[1,2] Oscar J. Abilez,[4] Peng Zhao,[1,2] Edouard G. Stanley,[3] Andrew G. Elefanty,[3] Murray Kwon,[5] David A. Elliott,[3] and Reza Ardehali[1,2,*]

[1]Division of Cardiology, Department of Internal Medicine, David Geffen School of Medicine at UCLA, 675 Charles E Young Drive South, Room 3645, Los Angeles, CA 90095, USA
[2]Eli and Edythe Broad Stem Cell Research Center, University of California, Los Angeles, CA 90095, USA
[3]Murdoch Children's Research Institute, The Royal Children's Hospital, Parkville, VIC 3052, Australia
[4]Bio-X Program, Cardiovascular Medicine, Cardiovascular Institute, Stanford University School of Medicine, Stanford, CA 94305, USA
[5]Division of Cardiothoracic Surgery, Department of Surgery, David Geffen School of Medicine at UCLA, Los Angeles, CA 90095, USA
*Correspondence: rardehali@mednet.ucla.edu
http://dx.doi.org/10.1016/j.stemcr.2015.11.006

SUMMARY

The generation of tissue-specific cell types from human embryonic stem cells (hESCs) is critical for the development of future stem cell-based regenerative therapies. Here, we identify CD13 and ROR2 as cell-surface markers capable of selecting early cardiac mesoderm emerging during hESC differentiation. We demonstrate that the CD13+/ROR2+ population encompasses pre-cardiac mesoderm, which efficiently differentiates to all major cardiovascular lineages. We determined the engraftment potential of CD13+/ROR2+ in small (murine) and large (porcine) animal models, and demonstrated that CD13+/ROR2+ progenitors have the capacity to differentiate toward cardiomyocytes, fibroblasts, smooth muscle, and endothelial cells in vivo. Collectively, our data show that CD13 and ROR2 identify a cardiac lineage precursor pool that is capable of successful engraftment into the porcine heart. These markers represent valuable tools for further dissection of early human cardiac differentiation, and will enable a detailed assessment of human pluripotent stem cell-derived cardiac lineage cells for potential clinical applications.

INTRODUCTION

The mammalian heart has been reported to possess a limited regenerative capacity; however, this is not sufficient to effectively remuscularize the heart after a myocardial infarction (MI) (Ali et al., 2014). In the case of severe MI the human heart experiences dramatic loss of cardiomyocytes, the basic functional unit of the heart, with estimates placing that loss upward of a billion cells (Bergmann et al., 2009; Laflamme and Murry, 2005). As heart disease continues to be a leading cause of mortality worldwide, the use of human pluripotent stem cells (hPSCs) for cardiac regeneration is a compelling approach and has become a major focus of stem cell research (Cibelli et al., 2013; Matsa et al., 2014). Indeed, the first human subject receiving hPSC-derived cardiovascular progenitors as a therapeutic for heart failure has recently been reported (Menasche et al., 2015).

The progression of in vitro-derived cardiac cells toward therapeutic applications will be greatly assisted by an increasingly detailed understanding of cardiac lineage commitment. Moreover, it is still unclear whether committed progenitors or fully differentiated cells will be most efficacious for any particular therapeutic use. Indeed, homogeneous populations of cardiovascular progenitor cells that have the capacity to form multiple cardiac cell types (e.g., cardiomyocytes, fibroblasts, and vascular cells) may have a role to play in future stem cell-based therapies. In this context, further research is required to elaborate the cardiac lineage tree and to devise methods for isolating key cell types and their progenitors.

Generation of a pure hPSC-derived cardiac population through an intermediate mesodermal germ layer (from which the cardiac tissue arises) may be of therapeutic importance. Previous studies have identified SSEA1, PDGFRα, and KDR as surface markers on PSC-derived mesodermal progenitors with capacity to generate cardiovascular lineages (Blin et al., 2010; Kattman et al., 2011; Yang et al., 2008). Subsequently, SIRPA and VCAM1 were identified as novel markers of cardiomyogenic lineages (Dubois et al., 2011; Elliott et al., 2011; Skelton et al., 2014; Uosaki et al., 2011). These studies provide a foundation upon which to construct a human cardiovascular cell lineage tree based on cell-surface markers, analogous to that of the hematopoietic system.

Other surface markers, such as CD13 and ROR2, have been used in combination with PDGFRα and KDR to isolate progenitors capable of giving rise to enriched cardiac cell populations (Ardehali et al., 2013). The combination of these four markers led to isolation of committed

cardiovascular cells as shown by in vitro and in vivo analyses. However, the utility of CD13 and ROR2 as standalone markers of cardiac intermediates remains unclear. Here, we define CD13 and ROR2 as markers of mesodermal progenitors of cardiac cell lineages. Furthermore, in vivo cardiac differentiation and engraftment efficiency of CD13+/ROR2+ cells was compared in large (porcine) and small (murine) animal models. Our data demonstrate that human embryonic stem cell-derived cardiovascular progenitor cells (hESC-CPCs) engraft and differentiate into all cardiovascular lineages more efficiently in the porcine heart than in the mouse heart. Consistent with previous reports, these data suggest that the murine heart may be an inappropriate xenotransplantation model (Cibelli et al., 2013; van Laake et al., 2008, 2009). The pig heart, however, may provide a useful pre-clinical platform upon which to test the regenerative potential of hESC-CPCs (Ye et al., 2014). Collectively, these findings enhance our understanding of cardiac mesoderm lineage formation, provide well-defined tools for the enrichment of cardiac-committed mesoderm, and demonstrate engraftment and differentiation of transplanted hESC-CPCs in porcine hearts.

RESULTS

CD13 and ROR2 Markers Can Be Used for Prospective Isolation of Pre-cardiac Mesoderm Cells

Initially, a stencil differentiation protocol (Myers et al., 2013) was used to isolate mesodermal cells based on GFP expression from the *MIXL1* locus (Davis et al., 2008) (Figure S1). Microarray analysis of isolated cells from day 3 of differentiation was used to identify differences between MIXL1^{eGFP+} and MIXL1^{eGFP-} transcriptomes. We identified 6,757 differentially regulated genes, of which 2,520 were upregulated $\geq$2-fold in the eGFP+ (MIXL1^{+}) mesoderm population (Figure 1A). These included known mesodermal markers, such as *T*, *PDGFRα*, *MESP1*, and *EOMES*, as well as two genes encoding for cell-surface proteins, *CD13* (an aminopeptidase) and *ROR2* (a Wnt receptor) (Figure 1A). To further investigate the expression profile of CD13 and ROR2, we differentiated *MIXL1*$^{eGFP/w}$ hESCs toward mesoderm and conducted flow cytometry analysis. On day 3 of differentiation, approximately 30% of cells co-expressed CD13 and ROR2 in several hPSC lines that were tested (Figure 1B). More efficient differentiation schemes using the H3 hESC line produced populations consisting upward of 80% CD13+/ROR2+ cells (Figures 1C, S2A, and S2B). Later in differentiation, the majority of cells downregulated CD13 while maintaining ROR2+ expression out to day 10 (~92%) (Figure 1C). Flow cytometry analysis also showed that approximately 70% of the eGFP+ (MIXL1^{+}) population expressed CD13 and ROR2 on day 3 of differentiation (Figure 1D). Comparatively, very few CD13+/ROR2+ (13R2+) cells were detected in the eGFP− (MIXL1^{-}) fraction (~4%) (Figure 1D), suggesting that CD13 and ROR2 are predominantly restricted to a mesoderm population marked by MIXL1 expression. In addition, qPCR analysis of 13R2+ cells confirmed the high expression levels of cardiac precursor markers such as *PDGFRα* (1.1×10^4-fold), *HAND1* (5.4×10^3-fold), *MESP1* (530-fold), and *EOMES* (1.4×10^4-fold) relative to *GAPDH* (Figure 1E). Subsequently, we performed expression profiling of triple-positive (MIXL1+/CD13+/ROR2+) and triple-negative (MIXL1−/CD13−/ROR2−) populations. Gene Ontology (GO) analysis revealed that the transcripts enriched in the MIXL1+/CD13+/ROR2+ population correlated with the processes of heart development ($p = 6.79 \times 10^{-10}$), germ layer formation ($p = 1.78 \times 10^{-6}$), gastrulation ($p = 2.77 \times 10^{-6}$), mesoderm development ($p = 5.52 \times 10^{-6}$), and heart morphogenesis ($p = 2.18 \times 10^{-5}$) (Figures 1F and 1G).

We next sought to determine whether CD13 and ROR2 are expressed on MIXL1+ endoderm-derived cells. Flow cytometric analysis of *MIXL1*$^{GFP/w}$ cells differentiated under endodermal conditions (D'Amour et al., 2005) revealed no substantial expression of CD13 or ROR2 on MIXL1-eGFP+ endoderm cells (Figure 2A). This observation was confirmed by qPCR, demonstrating a 26- and a 2-fold decrease in the expression of CD13 and ROR2, respectively, relative to mesodermal MIXL1-eGFP+ cells (Figure 2B). Furthermore, throughout differentiation 13R2+ cells expressed low levels of endodermal markers, including *SOX17*, *SOX7*, *FOXA2*, and *HFN4A*, relative to the CD13−/ROR2− fraction (Figure 2C). To confirm the restriction of CD13 and ROR2 expression to mesoderm-derived cells, we tested for the presence of the definitive endoderm cell-surface marker, CXCR4 (McGrath et al., 1999; Yusuf et al., 2005). Flow cytometric analysis of mesoderm cells derived from unmodified H9 hESCs revealed that expression of CXCR4 and CD13/ROR2 is mutually exclusive (Figure 2D). This differential expression pattern was further confirmed by immunofluorescence staining (Figures 3A and S2C). 13R2+ cells also downregulated pluripotency markers, and expressed the cardiac mesoderm markers MESP1 and MIXL1 (88% ± 2.3% SEM, n = 3) (Figures 1E, 1F, 2C, 3A, S2D, and S2E). Together, these results indicate that CD13 and ROR2 can be used to preferentially select for mesoderm from a mixed population of differentiating hESCs.

In accordance with previous reports that an epithelial-to-mesenchymal transition (EMT) occurs at an early stage of mesoderm commitment, we analyzed the expression of EpCAM/CD326 and NCAM/CD56 in 13R2+ fractions (Evseenko et al., 2010). We observed that approximately 90% of sorted 13R2+ cells expressed CD56 and downregulated CD326 after 2 days of reculture, suggestive of an EMT

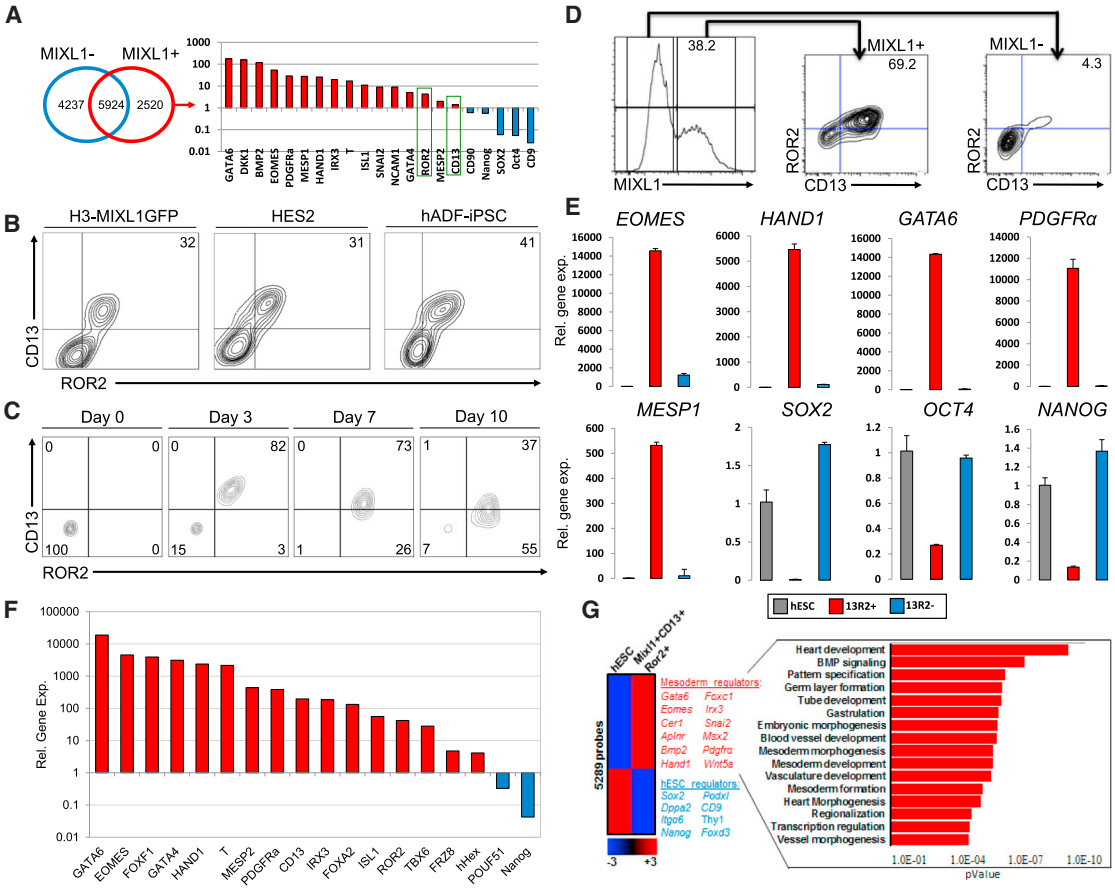

Figure 1. CD13 and ROR2 Mark the Mesoderm

(A) Microarray analysis comparing the transcriptomes of MIXL1eGFP fractions reveals upregulation of CD13 (overall rank 1,230) and ROR2 (overall rank 564) as two surface markers in the mesodermal fraction.

(B) Day-3 flow cytometry analysis detailing CD13 and ROR2 expression in H3-MIXL1eGFP, hES2, and iPS cell lines.

(C) Flow cytometry analysis time course detailing expression of CD13 and ROR2 at days 0, 3, 7, and 10 of an efficient monolayer differentiation. See also Figures S2A and S2B.

(D) Day-3 flow cytometry analysis showing CD13 and ROR2 expression in MIXL1+ and MIXL1 fractions.

(E) Day-3 qPCR analysis of CD13+/ROR2+ and CD13+/ROR2− cells in comparison with hESCs (n = 3; ±SEM).

(F) Single-gene qPCR analysis of the Mixl1^{eGFP+}/CD13+/ROR2+ population showing expression levels of mesoderm-associated genes and pluripotent genes (n = 1).

(G) Gene ontology analysis of Mixl1^{eGFP+}/CD13+/ROR2+ detailing association with heart formation and mesoderm lineage development. n represents the number of individual experiments in all instances.

process and mesoderm specification (Figure 3B). Comparatively, the CD13−/ROR2− (13R2−) fraction was largely CD56−/CD326+ (~87%), consistent with an epithelial phenotype (Figures 3B and S2F). A proportion of the day-3 CD13+ and 13R2+ fraction also expressed PDGFRα (45.7% ± 2.1%, n = 3) and C-KIT (1.3% ± 0.8%, n = 3), respectively (Figures S3A and S3B). Furthermore, 18.8% ± 6.4% (n = 3) of the ROR2+ fraction expressed KDR (Figure S3C). Nonetheless, a large majority of day-3 13R2+ cells were negative for SSEA1 (Figure S3E). Surface markers associated with later stages of cardiac differentiation were also absent from the 13R2+ population, including VCAM1, SIRPA, and CD34 (Figures S3F and S3G). Collectively, these data suggest that CD13 and ROR2 mark a distinct, transitory state of EMT committed cells and can be used to prospectively enrich for pre-cardiac mesoderm, depleting both endodermal and residual pluripotent cells.

CD13+/ROR2+ Cells Give Rise to Cardiomyocytes, Smooth Muscle, and Endothelium In Vitro

Next, we sought to determine the efficiency at which purified 13R2+ cells differentiate toward definitive cardiovascular lineages. To assist downstream characterization, we generated a double reporter hESC line in which eGFP

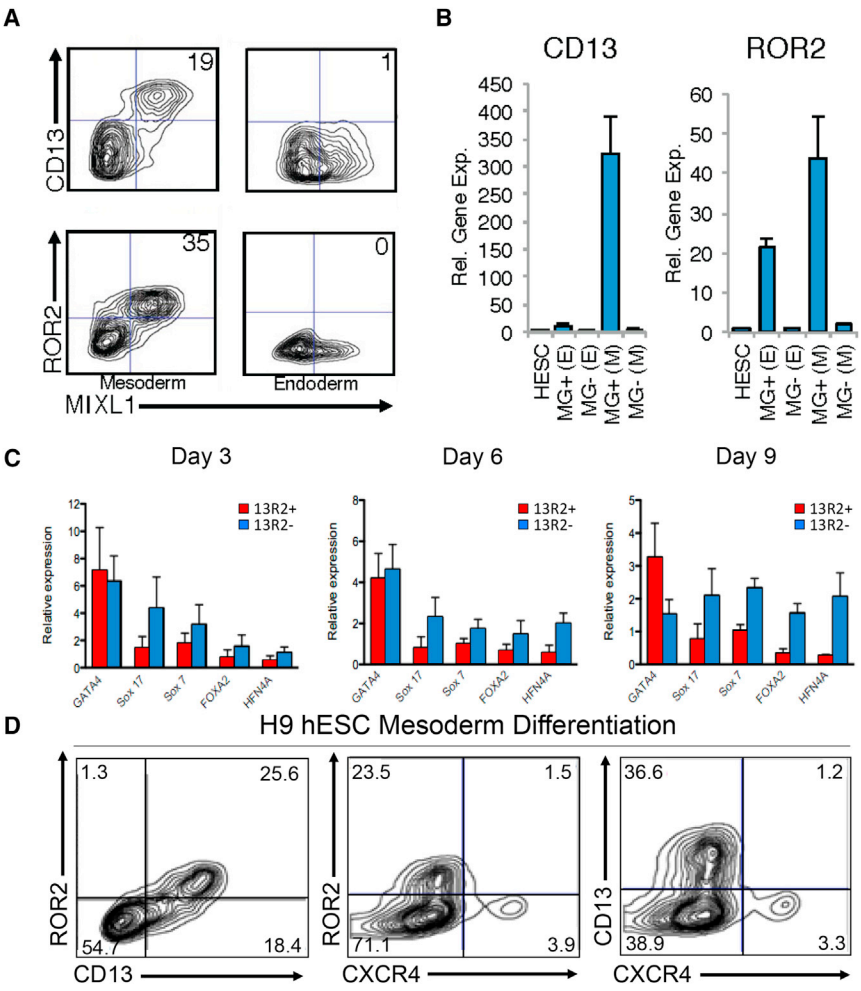

Figure 2. CD13 and ROR2 Preferentially Select Mesoderm and Deplete Endoderm

(A) Day-3 flow cytometry analysis showing expression of CD13, ROR2, and MIXL1-eGFP in mesoderm and endoderm differentiations.

(B) Day-3 qPCR analysis detailing expression of CD13 and ROR2 in hESCs, MIXL1+ (MG+), and MIXL1− (MG-) cells from endoderm (E) and mesoderm (M) differentiations (n = 3; ±SEM).

(C) qPCR analysis detailing endodermal gene expression in CD13/ROR2 fractions sorted at days 3, 6, and 9 of differentiation.

(D) Day-3 flow cytometry analysis of unmodified H9 mesoderm differentiation showing co-expression of ROR2/CD13, but not ROR2/CXCR4 or CD13/CXCR4.

n represents the number of individual experiments in all instances.

is expressed upon activation of endogenous NKX2-5 (Elliott et al., 2011) and mCherry expression is controlled by the αMHC promoter (Kita-Matsuo et al., 2009). This dual-color hESC line facilitates identification and quantification of cardiac progenitors and cardiomyocytes based upon expression of *NKX2-5* and *αMHC*, respectively. Sorted 13R2− cells did not survive in our monolayer differentiation protocols for the extended time period required for analysis, so unsorted cells served as a control.

Isolated 13R2+ cells were recultured under conditions promoting cardiomyocyte differentiation to characterize their developmental potential. Seven days post sort, 86% ± 3.2% (n = 3) of 13R2+ cells proceeded to express NKX2-5eGFP, compared with 22% ± 4.9% (n = 3) in the unsorted population (Figure 4A). Furthermore, 63% ± 4.1% (n = 3) of 13R2+ cells differentiated to express mCherry in addition to eGFP (indicating progression to cardiomyocytes), whereas only 16% ± 4.0% (n = 3) of the unsorted population was observed to be eGFP+/mCherry+ (Figures 4A and S4A). Although differentiation efficiency varied significantly in unsorted cells, we observed a persistently high rate of cardiomyocyte generation when selecting for CD13/ROR2. Gene expression analysis supported these findings, and demonstrated that differentiating 13R2+ cells temporally expressed high levels of cardiac mesoderm genes followed by cardiovascular progenitor and definitive cardiomyocyte genes (Figures 4B and S4B). This was illustrated by elevated expression levels of *HAND1* and *MIXL1* at day 4, followed by *ISL-1*, *MEF2C*, *TBX5*, and *NKX2-5* by days 7–10, and *cTnT*, *MYL2*, *IRX4*, and *NPPA* at later stages (Figures 4B and S4B). In addition, when we analyzed expression of eGFP and mCherry on days 7 and 14 as markers for NKX2-5 and αMHC, respectively, we noted higher expression levels in 13R2+ cells when compared with either day-3 sorted single positive CD13 or ROR2, day-4 sorted SSEA1+, and day-5 sorted PDGFR+/KDR+ populations (Figures S4C–S4H). Furthermore, when maintained in a monolayer culture, 13R2+ cells displayed cardiac troponin T (cTnT)-positive sarcomeric structures, and formed contractile 3D layers (Figures 4C and Movie S1).

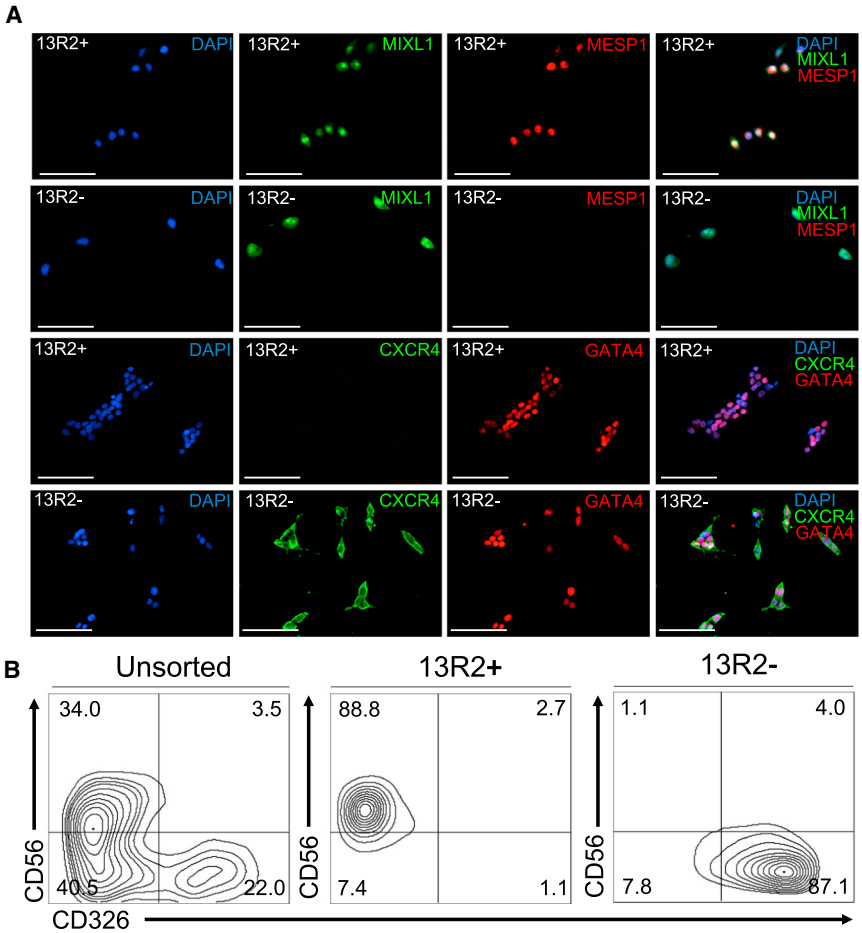

Figure 3. CD13 and ROR2 Mark a Distinct, Transitory Pre-cardiac Mesoderm Population

(A) Day-4 ICC analysis of sorted 13R2+ and 13R2− cells from hESC mesoderm differentiations, showing expression of MIXL1, MESP1, CXCR4, and GATA4. Scale bars, 25 μm. See also Figures S2C and S2D.

(B) Day-5 flow cytometric analysis of unsorted and sorted 13R2+ and 13R2− cells for expression of CD326 and CD56. See also Figure S2F.

Together, these results suggest that 13R2+ cells give rise to a highly enriched population of cardiomyocytes.

We next sought to determine whether 13R2+ cells can give rise to other cardiovascular lineages. Under cardiomyocyte culture conditions, a proportion of the day-3 sorted 13R2+ fraction progressed toward an αSMA+ phenotype (Figure 4C). Furthermore, the expression level of smooth muscle transcripts, *ACTA2* (*αSMA*) and *CNN1*, were significantly higher in 13R2+ cells at various time points during days 7–14 of differentiation ($p < 0.05$) (Figure 4D). To further investigate the lineage potential of the 13R2+ fraction, we cultured day-3 sorted 13R2+ cells under conditions to promote smooth muscle differentiation (transforming growth factor β 2 ng/ml, platelet-derived growth factor β 10 ng/ml) (Cheung et al., 2014). After 11 days in culture, 13R2+ cells expressed high levels of *ACTA2* (*αSMA*) and *CNN1* transcripts, and low levels of *VE-cadherin*, consistent with a smooth muscle phenotype (Figure 4E). Enrichment for smooth muscle cells in the differentiated 13R2+ population was confirmed by protein-level expression of αSMA and CNN1, as determined by immunocytochemistry (ICC) (Figure S4I).

A fraction of 13R2+ cells also differentiated toward a VE-cadherin+ phenotype in standard cardiomyocyte differentiations (Figure 4C). To further characterize endothelial differentiation, we cultured day-3 sorted 13R2+ cells under endothelial conditions (50 ng/ml vascular endothelial growth factor, 20 ng/ml stem cell factor, 10 ng/ml basic fibroblast growth factor). After 11 days of culture under these conditions, 13R2+ cells expressed high levels of the endothelial markers *VE-cadherin*, *TAL1*, *TEK*, *KDR*, and *vWF* (Figure 4E). Furthermore, after 14 days flow cytometric analysis revealed that a subset of sorted 13R2+ cells proceeded to co-express CD31/CD34 and CD31/KDR (32% and 37%, respectively), consistent with an endothelial phenotype (Figures 4F and S4J). Taken together, these results suggest that 13R2+ cells on day 3 of differentiation represent cardiovascular mesoderm capable of giving rise to cardiomyocytes, smooth muscle, and endothelial cells.

Temporal Gene Expression Profiling of CD13+/ROR2+ Cells and Their Progeny

To determine the gene expression profile at different stages of cardiac differentiation from hESCs, we performed

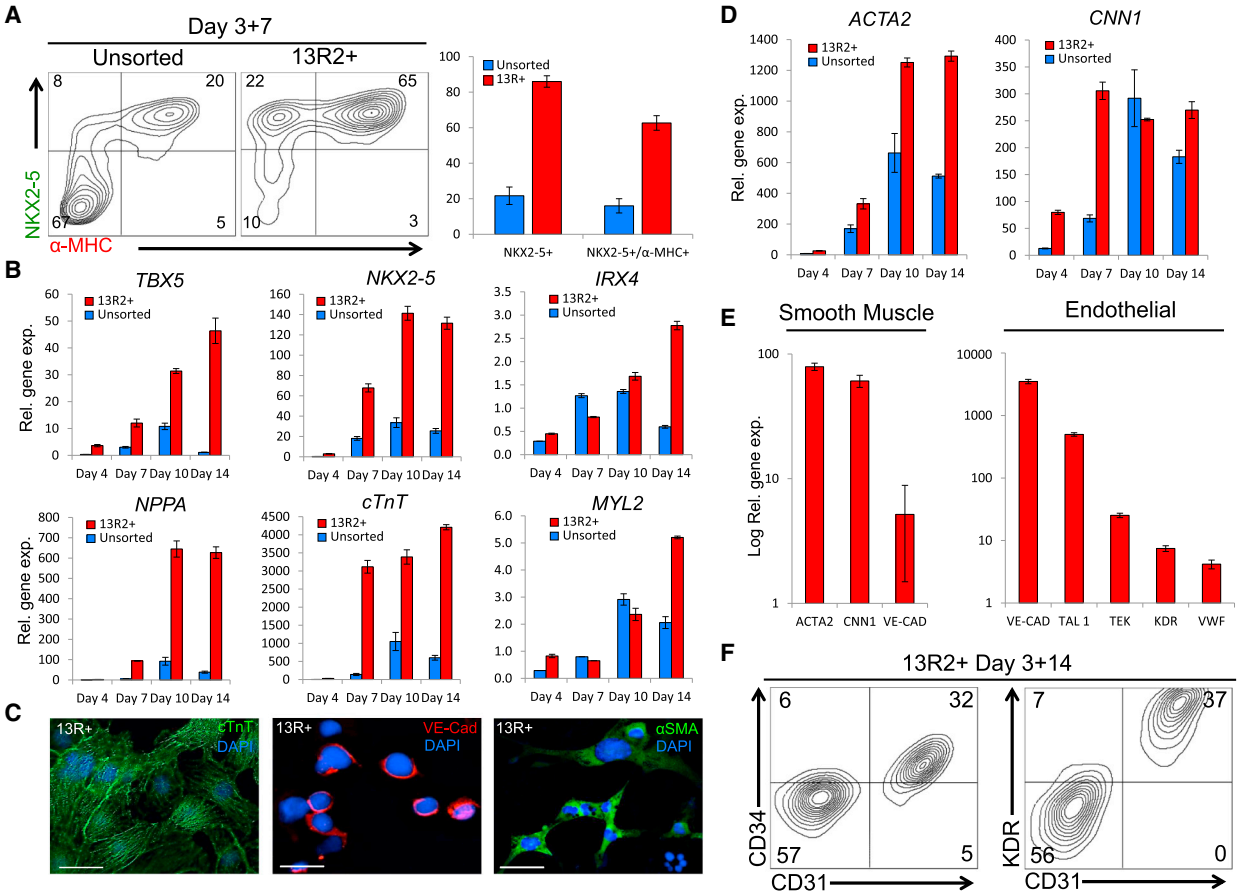

Figure 4. CD13+/ROR2+ Cells Give Rise to Enriched Cardiomyocyte Populations and Differentiate toward Endothelial and Smooth Muscle Cells

(A) Day-10 flow cytometric analysis of day-3 sorted 13R2+ and unsorted cells showing expression of NKX2-5eGFP and αMHC-mCherry (n = 3; ±SEM). See also Figure S4A.

(B) qPCR time course detailing the expression of cardiac mesoderm and definitive cardiomyocyte genes over 14 days of differentiation relative to GAPDH (n = 3; ±SEM). See also Figure S4B.

(C) Immunofluorescence analysis of 13R2+ cells after 12 days in culture for markers of cardiomyocytes (cTnT), endothelial (VE-cadherin), and smooth muscle cells (αSMA). Scale bars, 10 μm.

(D) qPCR analysis of smooth muscle genes over 14 days of differentiation in unsorted and sorted 13R2+ cell fractions, relative to GAPDH (n = 3; ±SEM).

(E) Day-14 qPCR analysis of endothelial and smooth muscle cultured 13R2+ cells relative to GAPDH (n = 3; ±SEM) (see also Figures S4I and S4J).

(F) Day-14 flow cytometry analysis of endothelial cultured 13R2+ cells showing co-expression of CD31/CD34 and CD31/KDR, respectively. n represents individual experiments in all instances.

transcriptome (RNA-seq) analysis on undifferentiated hESCs, 13R2+ and 13R2− populations from day 3, 13R2+/NKX2-5+, and 13R2+/NKX2-5− from day 7, and 13R2+/NKX2-5+/αMHC+ and 13R2+/NKX2-5+/αMHC− from day 14 (Figure S5). These data supported previous findings showing an enrichment of pre-cardiac mesodermal genes and concomitant downregulation of pluripotency genes in the 13R2+ population on day 3 (Figure 5A). Day-7 13R2+/NKX2-5+ cells expressed cardiac transcription factors such as *MEF2-C*, *NKX2-5*, *TBX20*, and *TBX5*, suggestive of commitment to a cardiac progenitor cell type (Figure 5A). Day-7 13R2+/NKX2-5+ cells were also enriched for cardiomyocyte markers *TNNT2*, *KCNIP2*, *KCNH7*, and *MYL4* (Figure 5A). The day-14 13R2+/NKX2-5+/αMHC+ fraction maintained expression of these cardiomyocyte markers, in addition to upregulating other cardiomyocyte genes such as *NPPA*, *NPPB*, *MYH7*, and *MYL7*, suggestive of a progression toward a more differentiated cardiomyocyte phenotype (Figure 5A). In addition, both day-14 13R2+/NKX2-5+/αMHC+ and 13R2+/NKX2-5+/αMHC− populations

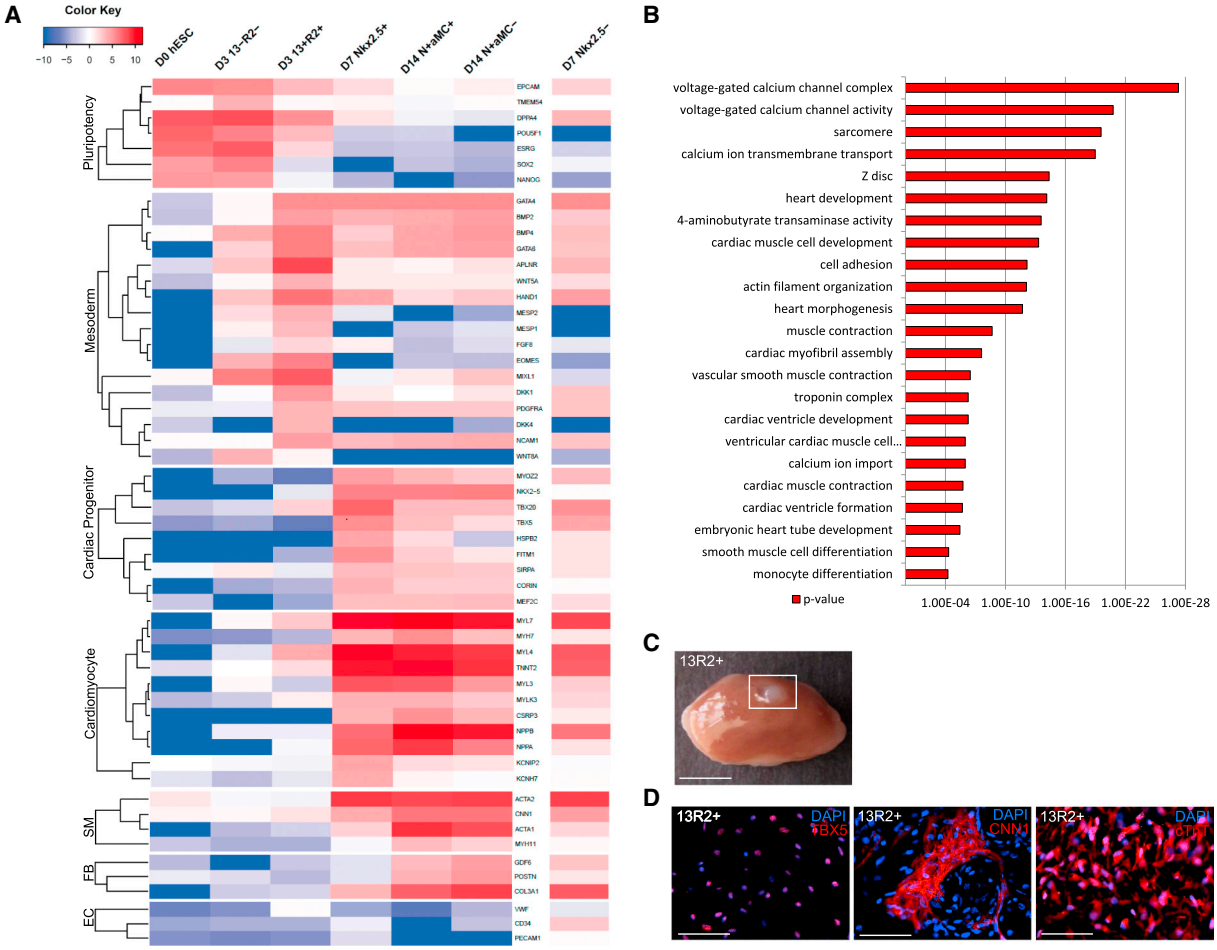

Figure 5. CD13+/ROR2+ Downstream Gene Ontology and In Vivo Kidney Capsule Differentiation

(A) RNA-seq time-course analysis of hESCs, day-3 13R2+ and 13R2− cells, day-7 13R2+-derived NKX2-5+ and NKX2-5− cells, day-14 13R2+/NKX2-5+-derived αMHC+ and αMHC− cells (see also Figure S5). Genes are grouped into seven categories, including pluripotency, mesoderm, cardiac progenitor, cardiomyocyte, smooth muscle (SM), fibroblast (FB), and endothelium (EC) (n = 1).

(B) GO analysis showing GO terms associated with upregulated gene expression in day-7 13R2+-derived NKX2-5+ and day-14 13R2+/NKX2-5+-derived αMHC+ populations.

(C and D) Gross anatomical (C) and immunohistochemistry (IHC) images (D) of kidney capsule sections 6 weeks after injection with 13R2+ cells. IHC images show expression of TBX5 (red), CNN1 (red), and cTnT (red), respectively. Nuclei are stained with DAPI (blue). Scale bars represent 5 mm (C) and 25 μm (D) (n = 3).

n represents the number of individual experiments in all instances.

were enriched for smooth muscle genes, such as *MYH11*, *CNN1*, and *ACTA1*, suggesting that these populations may also contain vascular smooth muscle cells (Figure 5A).

GO analysis of the upregulated transcripts in day-7 13R2+/NKX2-5+ and day-14 13R2+/NKX2-5+/αMHC+ fractions generated a list of 100 GO terms with $p < 0.0005$. These included voltage-gated calcium channels ($p = 4.9 \times 10^{-26}$), heart morphogenesis ($p = 1.56 \times 10^{-12}$), muscle contraction ($p = 2.15 \times 10^{-9}$), myofibril assembly ($p = 2.46 \times 10^{-8}$) and calcium ion transport ($p = 1.04 \times 10^{-6}$), further confirming the progression of 13R2+ progenitors toward cardiac cell types, and in particular cardiomyocytes (Figure 5B). The transcriptional profile of CD13/ROR2 fractions and their progeny maps out the developmental hierarchy of a putative pre-cardiac mesodermal cell population that differentiates to cardiac progenitors with subsequent specification to mature cardiomyocytes.

Transplantation of CD13/ROR2 Cells in a Murine Model

To determine whether 13R2+ cells retain an in vivo latent potential to differentiate to a cardiovascular lineage, we transplanted these cells into the mouse kidney capsule

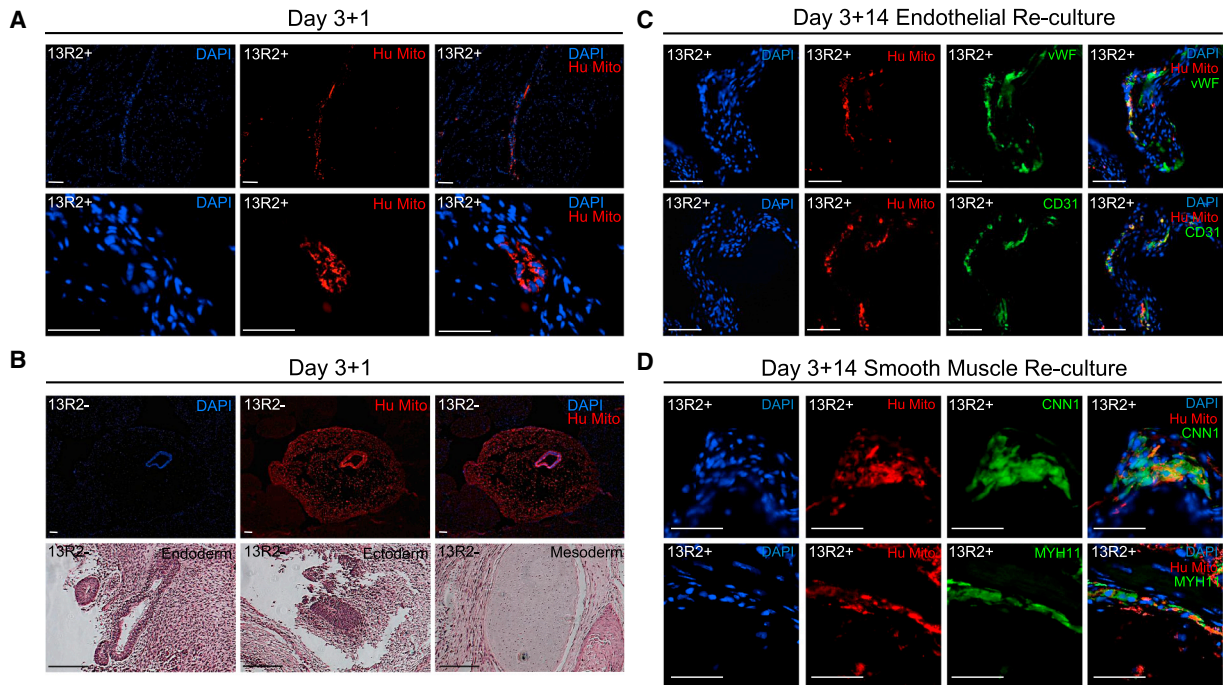

Figure 6. In Vivo Differentiation and Engraftment of CD13+/ROR2+ Cells in the Mouse Heart

(A) IHC analysis of explanted mouse hearts 6 weeks after injection with 13R2+ cells showing staining for human mitochondria (red). Nuclei are stained with DAPI (blue). Scale bars, 100 μm (n = 6). See also Figure S6.

(B) IHC analysis of explanted mouse hearts 6 weeks after injection with 13R2− cells showing staining for human mitochondria (red). Nuclei are stained with DAPI (blue). Scale bars, 200 μm (see also Figure S6A). IHC H&E staining of 13R2− cell-derived teratomas is also shown (see also Figure S6A). Scale bars, 200 μm (n = 6). See also Figure S6.

(C) IHC analysis of explanted mouse hearts 6 weeks after injection with endothelially directed 13R2+ cells showing expression of human mitochondria (red), vWF (green), and CD31 (green), respectively. Nuclei are stained with DAPI (blue). Scale bars, 25 μm (n = 6).

(D) IHC analysis of explanted mouse hearts 6 weeks after injection with smooth muscle-directed 13R2+ cells showing expression of human mitochondria (red), CNN1 (green), and MYH11 (green), respectively. Nuclei are stained with DAPI (blue). Scale bars, 25 μm (n = 6).

n represents the number of individual experiments in all instances.

and heart. Day-3 13R2+ cells were isolated from a differentiating *NKX2-5*$^{GFP/w}$ hESC reporter line (Elliott et al., 2011), recovered for 24 hr in culture, and approximately 5 × 10^5 cells were implanted under the kidney capsule of non-obese diabetic/SCID mice with common γ-chain knockout (NSG) (Figure 5C). Six weeks later, 13R2+ grafts had eGFP+ patches demonstrating NKX2-5 expression. Transplanted 13R2+ progeny also contained cells expressing cardiac progenitor (TBX5), smooth muscle (CNN1), and cardiomyocyte (cTnT) proteins (Figure 5D). However, these grafts were not contractile and did not form organized sarcomeric structures. Furthermore, transplanted 13R2+ cells did not express the endothelial markers CD31 and APJ. These data indicate that the mouse kidney capsule may not provide a supportive environment for human myocardial or endothelial differentiation.

Differentiation potential of day-3 13R2+ cells was also tested in the mouse heart. Approximately 5 × 10^5 13R2+ (or 13R2−) cells were sorted and recultured for 24 hr before transplantation by direct injection into the left ventricle of healthy NSG mouse hearts, or into the peri-infarct area following occlusion of the left anterior coronary descending artery (n = 6 in each group). Control experiments included equivalent volumes of conditioned media administered in similar locations of healthy and injured mouse hearts (n = 6). Engraftment was examined 8 weeks after transplantation by screening for human mitochondria staining in sectioned hearts (Figure 6). We detected very limited survival and engraftment of transplanted 13R2+ cells in the healthy NSG mouse hearts, and no substantial human cells in injured hearts. Engrafted 13R2+ cells did not express markers of definitive cardiac cell lineages, and no teratomas were observed (Figure 6A). Conversely, transplanted 13R2− cells formed teratomas, with mesoderm, endoderm, and ectoderm derivatives, in healthy (two of six) and injured (one of six) mouse hearts, suggesting the presence of residual undifferentiated hESCs (Figures 6B and S6A). Cardiac function, assessed by echocardiography

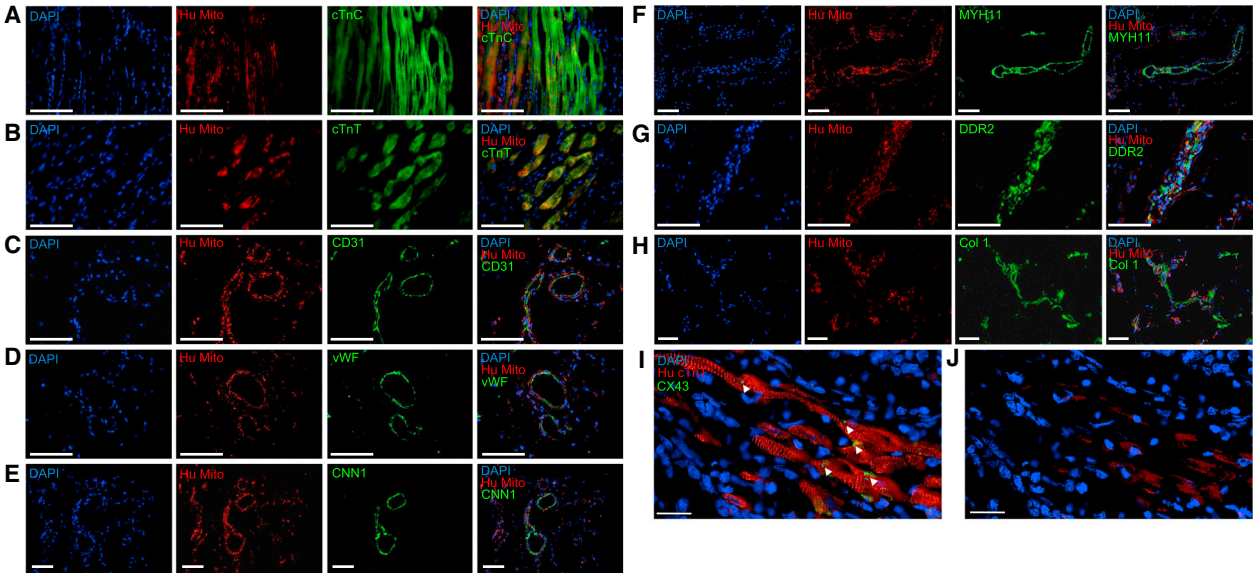

Figure 7. Transplanted CD13+/ROR2+ Cells Can Engraft and Differentiate in Pig Hearts

(A–H) Myocardial sections from porcine hearts 40 days after transplantation of 13R2+ cells show clusters of hESC-derived cardiovascular cells (see also Figure S7). IHC stains depict the expression human mitochondria (red), as well as cTnC (A), cTnT (B), CD31 (C), vWF (D), CNN1 (E), MYH11 (F), DDR2 (G), and Col 1 (H) (green), respectively. Nuclei are stained with DAPI (blue). Scale bars, 50 μm (n = 3). See also Figures S7B–S7E.

(I and J) A cluster of hESC-derived cardiomyocytes marked by human mitochondria (red) and cTnT (red) that demonstrates diffuse expression of Connexin 43 (green, marked by white arrowheads) between the transplanted cells. Scale bars, 20 μm (n = 3).

n represents the number of individual experiments in all instances.

at baseline and 8 weeks after intervention, revealed no changes in the ejection fraction or fractional shortening between groups (sham, conditioned media, 13R2+, or 13R2− transplants; n = 6 in each group) (Figure S6B).

While several studies have examined hESC-derived cardiomyocytes in murine hearts, less is known of the capacity of human smooth muscle and endothelial cells to improve heart function, possibly by neovascularization of the damaged tissue (Li et al., 2009; Xiong et al., 2012). We transplanted a total of approximately 5×10^5 smooth muscle and/or endothelial cells (derived from pre-sorted 13R2+ cells after 17 days in culture) into healthy and peri-infarcted areas of NSG mouse hearts (n = 12 in each group). Control experiments included equivalent volumes of conditioned media administered in similar locations of healthy and injured mouse hearts (n = 6). We observed rare hESC-derived vascular smooth muscle or endothelial cell engraftment in the injured mouse hearts. In healthy mouse hearts, very few 13R2+ cells successfully engrafted and expressed the endothelial markers vWF and CD31 (Figure 6C), or smooth muscle markers CNN1 and MHY11 (Figure 6D), respectively. No difference in cardiac function, based on echocardiographic measurements, was observed between treatments, i.e. sham, conditioned media, or cell transplantation (Figure S6C). Collectively these results indicate that the mouse heart, particularly after MI, may not provide a supportive niche for the engraftment of hESC-derived populations enriched for cardiovascular cells. Nevertheless, terminally differentiated 13R2+-derived smooth muscle and endothelium can engraft into the uninjured mouse heart, albeit at a very low frequency. Taken together, these mouse studies highlight the necessity to establish a clinically relevant large animal model to investigate transplantation of hESC-derived CPCs.

CD13+/ROR2+ Cells Engraft and Differentiate toward Cardiomyocytes, Endothelium, Smooth Muscle, and Fibroblasts in Pig Hearts

To provide a more relevant model to test the 13R2+ cell type for cardiac regeneration, we used a porcine model. Approximately 40×10^6 13R2+ cells were transplanted by direct injection into the left ventricle of healthy Yorkshire pig hearts, which remained on immunosuppressive therapy for the duration of the study (Figure S7A). The animals were euthanized after 40 days, and histological analyses of the explanted hearts showed numerous clusters of cells varying in size (5 to >1,000) staining positive for human mitochondria (Figures S7B–S7E; Figure 7A). Transplanted 13R2+ cells also expressed markers of cardiomyocytes (cTnC, cTnT) (Figures 7A and 7B), vascular endothelium

(CD31, vWF) (Figures 7C and 7D), smooth muscle cells (CNN1, MYH11), (Figures 7E and 7F), and fibroblasts (DDR2, Col1) (Figures 7G and 7H). In addition, we observed expression of CX43 between transplanted 13R2+-derived cardiomyocytes (Figures 7I and 7J). We did not detect the presence of CX43 between the graft and host myocardium. hESC-derived cardiomyocytes had highly organized myofibrils aligned with the host myocardium, suggestive of a maturing cardiomyocyte phenotype (Figures 7A, 7B, and 7I). Furthermore, 13R2+-derived endothelial and vascular smooth muscle cells contributed to vessel formation (Figures 7C–7F). No teratomas were observed in any of the animals transplanted with 13R2+ cells. Furthermore, no CD45+ cells were found near the engrafted hESC-derived cells, suggesting absence of immune cell infiltration to the graft site at the time of histological examination. However, consistent with other studies, we noted that the majority of the transplanted cells (>90%) were not retained in the recipient hearts (Ardehali et al., 2013; Blin et al., 2010; Chong et al., 2014; Mani et al., 2008; Tallheden et al., 2006; Thu et al., 2012; Ye et al., 2014). It should also be noted that we observed a small fraction of the 13R2+ transplanted cells within the heart that did not express any cardiovascular markers (approximately 10%–20%) and remained isolated from the surrounding host tissue (Figure S7C). Nonetheless, these data suggest that hESC-derived 13R2+ cells are capable of engrafting in the pig myocardium and differentiating toward cardiomyocytes, vascular endothelial cells, smooth muscle cells, and fibroblasts.

DISCUSSION

The identification of CD13 and ROR2 as early cardiogenic markers contributes to the establishment of a detailed cardiac lineage fate map and may subsequently aid developmental studies. Other cell-surface markers for isolation of mesoderm and cardiac progenitors have previously been reported (Ardehali et al., 2013; Blin et al., 2010; Drukker et al., 2012; Kattman et al., 2011; Skelton et al., 2014; Yang et al., 2008). Two such mesodermal markers for the isolation of cardiovascular progenitors from hESCs are PDGFRα and KDR (Ardehali et al., 2013; Kattman et al., 2011). However, not all cells selected by these markers are committed to the cardiovascular fate (Kattman et al., 2011). Furthermore, it was recently reported that MESP1+ cardiac mesoderm populations are enriched for PDGFRα+ and CD13+/ROR2+, but not PDGRRα+/KDR+ progenitors (Den Hartogh et al., 2015). This suggests that CD13 and ROR2 may mark a subset of cardiac mesoderm separate to that of the PDGFRα+/KDR+ fraction. Our results support these findings, as at day 3 of differentiation just under half of CD13+ cells co-expressed PDGFRα, and a small percentage (18.8% ± 6.4%, n = 3) of ROR2+ cells were KDR positive. In addition, very few 13R2+ cells expressed SSEA1 (0.3% ± 0.25%, n = 3) on day 3, supporting the notion that multiple progenitor subsets may exist at early stages of hESC cardiac differentiation. However, this may be due to the slight differences that exist between the expression patterns of these markers, with CD13/ROR2 being most highly upregulated at day 3, SSEA1 at day 4 (Blin et al., 2010), and PDGFRα/KDR at day 5 (Kattman et al., 2011) of cardiac differentiation. Further investigation is required to determine the temporal expression profile of these markers during cardiovascular differentiation.

Our results indicate that CD13 and ROR2 can be used to separate mesoderm from endoderm in a MIXL1+ background. It was noted that the day-4 CD13−/ROR2− population largely consists of a MIXL1+/MESP1−/GATA4+/CXCR4+ cell type, consistent with an endodermal phenotype. Throughout differentiation, the CD13−/ROR2− fraction also expressed high levels of endoderm markers, such as *SOX17*, *SOX7*, *FOXA2*, and *HFN4A*. Thus, at later stages of differentiation CD13 and ROR2 may have utility as negative selection markers for endoderm. However, at day 3 of differentiation the CD13−/ROR2− population also contained residual pluripotent cells that led to teratoma formation in the mouse hearts.

Flow cytometry data revealed a high degree of overlap between the surface expression of CD13 and ROR2. Few studies have detailed CD13 and ROR2 expression in the context of early cardiac development. Thus, it remains difficult to determine whether CD13/ROR2 co-expression in pre-cardiac mesoderm is coincidental, or due to a requirement for both in a shared (or interacting) developmental pathway(s). CD13 and ROR2 have biologically diverse roles, with CD13 commonly being associated with hematopoiesis and cancer (Dalal et al., 2014; Estey, 2013; Gorczyca et al., 2011; Zhang et al., 2011), and ROR2 regulating cellular processes via non-canonical Wnt signaling, with mutations in *ROR2* leading to Robinow syndrome (Afzal et al., 2000; Minami et al., 2010; Oishi et al., 2003). While this study shows that CD13 and ROR2 are expressed on a transitory population of early pre-cardiac mesodermal cells, their precise role in cardiac specification, if any, remains to be determined.

The application of surface markers to isolate pure tissue-specific progenitors offers several advantages for cell transplantation. First, it allows for isolation of a highly enriched, lineage-committed progenitor population. Second, it eliminates residual undifferentiated cells with the potential to form teratomas upon transplantation. Finally, it allows for a detailed investigation to delineate the developmental potential of progenitors after transplantation into the host. Successful transplantation of hESC-derived

cardiomyocytes has been reported in rodents (Ardehali et al., 2013; Ban et al., 2013; Hattori et al., 2010), guinea pigs (Shiba et al., 2012), and non-human primate models of myocardial ischemia (Blin et al., 2010; Chong et al., 2014). In contrast to some previous studies using more committed cell types, we did not identify any hESC-derived cardiomyocytes after transplantation of 13R2+ cardiac progenitors in the healthy or injured hearts of SCID mice. This may be due to the poor engraftment of the less mature, mesodermal 13R2+ cell type. After transplanting hESC-derived endothelial and smooth muscle cells into the mouse heart, we observed rare engraftment, representing less than 0.1% of total transplanted cells. Consistent with previous reports, no long-term cardiac functional improvement was observed in mice treated with hESC-derived cells (van Laake et al., 2007, 2008, 2009). Other groups have yielded more positive results using species-matched induced PSC (iPSC)-derived cardiac progenitors (Lalit et al., 2014; Mauritz et al., 2011; Pasha et al., 2011). For instance, Mauritz et al. (2011) observed that murine iPSC-derived Flk-1+ progenitors were capable of engrafting and functionally improving injured mouse heart. Thus, the observed lack of engraftment and differentiation by hESC-CPCs may be partially due to the inherent differences between mice and humans, reaffirming the importance of appropriate animal models for pre-clinical cardiac cell therapy development.

The pig has many advantages over mouse models for pre-clinical studies involving hESC-CPC transplantation, namely its similar heart size and physiology to human. In addition, pig cardiomyocytes have been shown to exhibit similar contraction rates and analogous action potential duration to humans (Stankovicova et al., 2000). We sought to determine whether CD13+/ROR2+ pre-cardiac mesodermal cells could engraft into the porcine myocardium and further differentiate into cardiovascular lineages. We chose to deliver 13R2+ cells into uninjured pig hearts to eliminate the many variables associated with the injury process. Extensive ICC analysis was performed, as in this context the *NKX2-5eGFP* and *αMHC-mCherry* fluorescence could not be reliably distinguished from the highly autofluorescent background. Our results indicated that many transplanted 13R2+ cells survived, engrafted, and differentiated toward definitive cardiovascular cell types in the pig heart after approximately 6 weeks. We observed small vessels that incorporated 13R2+-derived endothelial and vascular smooth muscle cells. In addition, we identified numerous areas within the pig's heart containing 13R2+-derived cardiomyocyte clusters ranging from 5 to >1,000 cells. Interestingly, many of these cells had organized sarcomere and formed Connexin-43 junctions between adjacent grafted cells. Whether 13R2+ cells are able to structurally and functionally integrate into the host myocardium and offer a therapeutic benefit to injured pig heart warrants further investigation. Such studies will be particularly important, given there is a negligible difference between the engraftment potential of hESC-derived cardiomyocytes and cardiac mesoderm (Chong et al., 2014). Ultimately, it is possible that combinations of different cell types (i.e. cardiomyocytes and cardiac progenitors) may improve graft survival and functional outcomes (Xiong et al., 2012; Ye et al., 2014).

In conclusion, this study demonstrates the utility of the cell-surface proteins CD13 and ROR2, which mark a population highly enriched for pre-cardiac mesoderm. Furthermore, we have shown that CD13+/ROR2+ cells are able to survive, engraft, and differentiate toward definitive cardiac cell types in pig, but not mouse hearts, highlighting the importance of clinically relevant animal models. Ultimately, the identification of CD13 and ROR2 as markers of early cardiac mesoderm may set the platform for future clinical trials for delivery of an enriched population of progenitors committed to the cardiovascular lineage without the risk of teratoma formation.

EXPERIMENTAL PROCEDURES

Maintenance of hESCs

Pluripotent *MIXL1-eGFP, NKX2-5eGFP,* and *NKX2-5eGFP/αMHC-mCherry hESC* lines were maintained as described previously (Davis et al., 2008; Pick et al., 2007).

Differentiation of hESCs

Cardiomyocyte monolayer differentiations were performed as previously described (Skelton et al., 2014).

Large Animal Cell Injection and Maintenance

Animal housing, maintenance, and experimentation were approved by and in accordance with guidelines set by the Institutional Animal Care and Use Committee of the University of California and the NIH Guide for the Care and Use of Laboratory Animals. A total of three 6- to 7-week-old Yorkshire pigs weighing approximately 40–45 kg underwent thoracotomy and transplantation of hESC-CPCs under direct visualization. Two injection sites were selected on the left ventricular free wall and marked with a suture. A suspension of 4×10^7 cells in approximately 300 μl of conditioned media was injected in each site using a 27-gauge needle. Pigs were immunosuppressed with cyclosporine (serum level maintained at 100–120 ng/ml), and treated with ketoconazole (20 mg/kg) and trimethoprim/sulfamethoxazole (40 mg/kg) daily, which began 3 days prior to cell transplantation until euthanasia. After 40 days the pigs were euthanized, and hearts were harvested and sectioned for histological analysis.

Statistical Analysis

Statistical testing was performed with Microsoft Excel version 12.2.8 and GraphPad Prism. Results are presented as mean ± SEM

and were compared using a two-tailed Student t test or two-way ANOVA (significance was assigned for $p < 0.05$). n represents the number of individual experiments in all instances.

Please refer to Supplemental Materials and Methods for full details of Experimental Procedures.

SUPPLEMENTAL INFORMATION

Supplemental Information includes Supplemental Materials and Methods, seven figures, two tables, and one movie and can be found with this article online at http://dx.doi.org/10.1016/j.stemcr.2015.11.006.

ACKNOWLEDGMENTS

The authors would like to thank all the members of the Ardehali laboratory for instructive discussions and suggestions. The authors would also like to thank the UCLA TRIC center and DLAM, namely Anthony Smithson, Sandra Duarte Vogel, and Janlee Jensen, for all their support and expertise in the handling of large animal models. Thanks are also due to the UCLA Flow Core, Namely Jessica Scholes and Felicia Codrea. Furthermore, the authors would like to especially thank Armin Hojjat, and Drs. Gay Crooks, Hanna Mikkola, and Thomas Vondriska for their valuable input and guidance. This work was supported in part by grants from the California Institute of Regenerative Medicine (CIRM) (RC1-00354-1) (R.A.) and Eli & Edith Broad Center of Regenerative Medicine and Stem Cell Research Center at UCLA Research Award (R.A.).

Received: June 19, 2015
Revised: November 14, 2015
Accepted: November 18, 2015
Published: January 12, 2016

REFERENCES

Afzal, A.R., Rajab, A., Fenske, C.D., Oldridge, M., Elanko, N., Ternes-Pereira, E., Tuysuz, B., Murday, V.A., Patton, M.A., Wilkie, A.O., et al. (2000). Recessive Robinow syndrome, allelic to dominant brachydactyly type B, is caused by mutation of ROR2. Nat. Genet. *25*, 419–422.

Ali, S.R., Hippenmeyer, S., Saadat, L.V., Luo, L., Weissman, I.L., and Ardehali, R. (2014). Existing cardiomyocytes generate cardiomyocytes at a low rate after birth in mice. Proc. Natl. Acad. Sci. USA *111*, 8850–8855.

Ardehali, R., Ali, S.R., Inlay, M.A., Abilez, O.J., Chen, M.Q., Blauwkamp, T.A., Yazawa, M., Gong, Y., Nusse, R., Drukker, M., et al. (2013). Prospective isolation of human embryonic stem cell-derived cardiovascular progenitors that integrate into human fetal heart tissue. Proc. Natl. Acad. Sci. USA *110*, 3405–3410.

Ban, K., Wile, B., Kim, S., Park, H.J., Byun, J., Cho, K.W., Saafir, T., Song, M.K., Yu, S.P., Wagner, M., et al. (2013). Purification of cardiomyocytes from differentiating pluripotent stem cells using molecular beacons that target cardiomyocyte-specific mRNA. Circulation *128*, 1897–1909.

Bergmann, O., Bhardwaj, R.D., Bernard, S., Zdunek, S., Barnabe-Heider, F., Walsh, S., Zupicich, J., Alkass, K., Buchholz, B.A., Druid, H., et al. (2009). Evidence for cardiomyocyte renewal in humans. Science *324*, 98–102.

Blin, G., Nury, D., Stefanovic, S., Neri, T., Guillevic, O., Brinon, B., Bellamy, V., Rucker-Martin, C., Barbry, P., Bel, A., et al. (2010). A purified population of multipotent cardiovascular progenitors derived from primate pluripotent stem cells engrafts in postmyocardial infarcted nonhuman primates. J. Clin. Invest. *120*, 1125–1139.

Cheung, C., Bernardo, A.S., Pedersen, R.A., and Sinha, S. (2014). Directed differentiation of embryonic origin-specific vascular smooth muscle subtypes from human pluripotent stem cells. Nat. Protoc. *9*, 929–938.

Chong, J.J., Yang, X., Don, C.W., Minami, E., Liu, Y.W., Weyers, J.J., Mahoney, W.M., Van Biber, B., Cook, S.M., Palpant, N.J., et al. (2014). Human embryonic-stem-cell-derived cardiomyocytes regenerate non-human primate hearts. Nature *510*, 273–277.

Cibelli, J., Emborg, M.E., Prockop, D.J., Roberts, M., Schatten, G., Rao, M., Harding, J., and Mirochnitchenko, O. (2013). Strategies for improving animal models for regenerative medicine. Cell Stem Cell *12*, 271–274.

D'Amour, K.A., Agulnick, A.D., Eliazer, S., Kelly, O.G., Kroon, E., and Baetge, E.E. (2005). Efficient differentiation of human embryonic stem cells to definitive endoderm. Nat. Biotechnol. *23*, 1534–1541.

Dalal, B.I., Al Mugairi, A., Pi, S., Lee, S.Y., Khare, N.S., Pal, J., Bryant, A., Vakil, A.P., Lau, S., and Abou Mourad, Y.R. (2014). Aberrant expression of CD13 identifies a subgroup of standard-risk adult acute lymphoblastic leukemia with inferior survival. Clin. Lymphoma Myeloma Leuk. *14*, 239–244.

Davis, R.P., Ng, E.S., Costa, M., Mossman, A.K., Sourris, K., Elefanty, A.G., and Stanley, E.G. (2008). Targeting a GFP reporter gene to the MIXL1 locus of human embryonic stem cells identifies human primitive streak-like cells and enables isolation of primitive hematopoietic precursors. Blood *111*, 1876–1884.

Den Hartogh, S.C., Schreurs, C., Monshouwer-Kloots, J.J., Davis, R.P., Elliott, D.A., Mummery, C.L., and Passier, R. (2015). Dual reporter MESP1 mCherry/w-NKX2-5 eGFP/w hESCs enable studying early human cardiac differentiation. Stem Cells *33*, 56–67.

Drukker, M., Tang, C., Ardehali, R., Rinkevich, Y., Seita, J., Lee, A.S., Mosley, A.R., Weissman, I.L., and Soen, Y. (2012). Isolation of primitive endoderm, mesoderm, vascular endothelial and trophoblast progenitors from human pluripotent stem cells. Nat. Biotechnol. *30*, 531–542.

Dubois, N.C., Craft, A.M., Sharma, P., Elliott, D.A., Stanley, E.G., Elefanty, A.G., Gramolini, A., and Keller, G. (2011). SIRPA is a specific cell-surface marker for isolating cardiomyocytes derived from human pluripotent stem cells. Nat. Biotechnol. *29*, 1011–1018.

Elliott, D.A., Braam, S.R., Koutsis, K., Ng, E.S., Jenny, R., Lagerqvist, E.L., Biben, C., Hatzistavrou, T., Hirst, C.E., Yu, Q.C., et al. (2011). NKX2-5(eGFP/w) hESCs for isolation of human cardiac progenitors and cardiomyocytes. Nat. Methods *8*, 1037–1040.

Estey, E.H. (2013). Acute myeloid leukemia: 2013 update on risk-stratification and management. Am. J. Hematol. *88*, 318–327.

Evseenko, D., Zhu, Y., Schenke-Layland, K., Kuo, J., Latour, B., Ge, S., Scholes, J., Dravid, G., Li, X., MacLellan, W.R., et al. (2010). Mapping the first stages of mesoderm commitment during differentiation of human embryonic stem cells. Proc. Natl. Acad. Sci. USA *107*, 13742–13747.

Gorczyca, W., Sun, Z.Y., Cronin, W., Li, X., Mau, S., and Tugulea, S. (2011). Immunophenotypic pattern of myeloid populations by flow cytometry analysis. Methods Cell Biol. *103*, 221–266.

Hattori, F., Chen, H., Yamashita, H., Tohyama, S., Satoh, Y.S., Yuasa, S., Li, W., Yamakawa, H., Tanaka, T., Onitsuka, T., et al. (2010). Nongenetic method for purifying stem cell-derived cardiomyocytes. Nat. Methods *7*, 61–66.

Kattman, S.J., Witty, A.D., Gagliardi, M., Dubois, N.C., Niapour, M., Hotta, A., Ellis, J., and Keller, G. (2011). Stage-specific optimization of activin/nodal and BMP signaling promotes cardiac differentiation of mouse and human pluripotent stem cell lines. Cell Stem Cell *8*, 228–240.

Kita-Matsuo, H., Barcova, M., Prigozhina, N., Salomonis, N., Wei, K., Jacot, J.G., Nelson, B., Spiering, S., Haverslag, R., Kim, C., et al. (2009). Lentiviral vectors and protocols for creation of stable hESC lines for fluorescent tracking and drug resistance selection of cardiomyocytes. PLoS One *4*, e5046.

Laflamme, M.A., and Murry, C.E. (2005). Regenerating the heart. Nat. Biotechnol. *23*, 845–856.

Lalit, P.A., Hei, D.J., Raval, A.N., and Kamp, T.J. (2014). Induced pluripotent stem cells for post-myocardial infarction repair: remarkable opportunities and challenges. Circ. Res. *114*, 1328–1345.

Li, Z., Wilson, K.D., Smith, B., Kraft, D.L., Jia, F., Huang, M., Xie, X., Robbins, R.C., Gambhir, S.S., Weissman, I.L., et al. (2009). Functional and transcriptional characterization of human embryonic stem cell-derived endothelial cells for treatment of myocardial infarction. PLoS One *4*, e8443.

Mani, V., Adler, E., Briley-Saebo, K.C., Bystrup, A., Fuster, V., Keller, G., and Fayad, Z.A. (2008). Serial in vivo positive contrast MRI of iron oxide-labeled embryonic stem cell-derived cardiac precursor cells in a mouse model of myocardial infarction. Magn. Reson. Med. *60*, 73–81.

Matsa, E., Burridge, P.W., and Wu, J.C. (2014). Human stem cells for modeling heart disease and for drug discovery. Sci. Transl. Med. *6*, 239ps236.

Mauritz, C., Martens, A., Rojas, S.V., Schnick, T., Rathert, C., Schecker, N., Menke, S., Glage, S., Zweigerdt, R., Haverich, A., et al. (2011). Induced pluripotent stem cell (iPSC)-derived Flk-1 progenitor cells engraft, differentiate, and improve heart function in a mouse model of acute myocardial infarction. Eur. Heart J. *32*, 2634–2641.

McGrath, K.E., Koniski, A.D., Maltby, K.M., McGann, J.K., and Palis, J. (1999). Embryonic expression and function of the chemokine SDF-1 and its receptor, CXCR4. Dev. Biol. *213*, 442–456.

Menasche, P., Vanneaux, V., Hagege, A., Bel, A., Cholley, B., Cacciapuoti, I., Parouchev, A., Benhamouda, N., Tachdjian, G., Tosca, L., et al. (2015). Human embryonic stem cell-derived cardiac progenitors for severe heart failure treatment: first clinical case report. Eur. Heart J. *36*, 2011–2017.

Minami, Y., Oishi, I., Endo, M., and Nishita, M. (2010). Ror-family receptor tyrosine kinases in noncanonical Wnt signaling: their implications in developmental morphogenesis and human diseases. Dev. Dyn. *239*, 1–15.

Myers, F.B., Silver, J.S., Zhuge, Y., Beygui, R.E., Zarins, C.K., Lee, L.P., and Abilez, O.J. (2013). Robust pluripotent stem cell expansion and cardiomyocyte differentiation via geometric patterning. Integr. Biol. (Camb) *5*, 1495–1506.

Oishi, I., Suzuki, H., Onishi, N., Takada, R., Kani, S., Ohkawara, B., Koshida, I., Suzuki, K., Yamada, G., Schwabe, G.C., et al. (2003). The receptor tyrosine kinase Ror2 is involved in non-canonical Wnt5a/JNK signalling pathway. Genes Cells *8*, 645–654.

Pasha, Z., Haider, H., and Ashraf, M. (2011). Efficient non-viral reprogramming of myoblasts to stemness with a single small molecule to generate cardiac progenitor cells. PLoS One *6*, e23667.

Pick, M., Azzola, L., Mossman, A., Stanley, E.G., and Elefanty, A.G. (2007). Differentiation of human embryonic stem cells in serum-free medium reveals distinct roles for bone morphogenetic protein 4, vascular endothelial growth factor, stem cell factor, and fibroblast growth factor 2 in hematopoiesis. Stem Cells *25*, 2206–2214.

Shiba, Y., Fernandes, S., Zhu, W.Z., Filice, D., Muskheli, V., Kim, J., Palpant, N.J., Gantz, J., Moyes, K.W., Reinecke, H., et al. (2012). Human ES-cell-derived cardiomyocytes electrically couple and suppress arrhythmias in injured hearts. Nature *489*, 322–325.

Skelton, R.J., Costa, M., Anderson, D.J., Bruveris, F., Finnin, B.W., Koutsis, K., Arasaratnam, D., White, A.J., Rafii, A., Ng, E.S., et al. (2014). SIRPA, VCAM1 and CD34 identify discrete lineages during early human cardiovascular development. Stem Cell Res. *13*, 172–179.

Stankovicova, T., Szilard, M., De Scheerder, I., and Sipido, K.R. (2000). M cells and transmural heterogeneity of action potential configuration in myocytes from the left ventricular wall of the pig heart. Cardiovasc. Res. *45*, 952–960.

Tallheden, T., Nannmark, U., Lorentzon, M., Rakotonirainy, O., Soussi, B., Waagstein, F., Jeppsson, A., Sjogren-Jansson, E., Lindahl, A., and Omerovic, E. (2006). In vivo MR imaging of magnetically labeled human embryonic stem cells. Life Sci. *79*, 999–1006.

Thu, M.S., Bryant, L.H., Coppola, T., Jordan, E.K., Budde, M.D., Lewis, B.K., Chaudhry, A., Ren, J., Varma, N.R., Arbab, A.S., et al. (2012). Self-assembling nanocomplexes by combining ferumoxytol, heparin and protamine for cell tracking by magnetic resonance imaging. Nat. Med. *18*, 463–467.

Uosaki, H., Fukushima, H., Takeuchi, A., Matsuoka, S., Nakatsuji, N., Yamanaka, S., and Yamashita, J.K. (2011). Efficient and scalable purification of cardiomyocytes from human embryonic and induced pluripotent stem cells by VCAM1 surface expression. PLoS One *6*, e23657.

van Laake, L.W., Passier, R., Monshouwer-Kloots, J., Verkleij, A.J., Lips, D.J., Freund, C., den Ouden, K., Ward-van Oostwaard, D., Korving, J., Tertoolen, L.G., et al. (2007). Human embryonic stem cell-derived cardiomyocytes survive and mature in the mouse heart and transiently improve function after myocardial infarction. Stem Cell Res. *1*, 9–24.

van Laake, L.W., Passier, R., Doevendans, P.A., and Mummery, C.L. (2008). Human embryonic stem cell-derived cardiomyocytes and cardiac repair in rodents. Circ. Res. *102*, 1008–1010.

van Laake, L.W., Passier, R., den Ouden, K., Schreurs, C., Monshouwer-Kloots, J., Ward-van Oostwaard, D., van Echteld, C.J., Doevendans, P.A., and Mummery, C.L. (2009). Improvement of mouse cardiac function by hESC-derived cardiomyocytes correlates with vascularity but not graft size. Stem Cell Res. *3*, 106–112.

Xiong, Q., Ye, L., Zhang, P., Lepley, M., Swingen, C., Zhang, L., Kaufman, D.S., and Zhang, J. (2012). Bioenergetic and functional consequences of cellular therapy: activation of endogenous cardiovascular progenitor cells. Circ. Res. *111*, 455–468.

Yang, L., Soonpaa, M.H., Adler, E.D., Roepke, T.K., Kattman, S.J., Kennedy, M., Henckaerts, E., Bonham, K., Abbott, G.W., Linden, R.M., et al. (2008). Human cardiovascular progenitor cells develop from a KDR+ embryonic-stem-cell-derived population. Nature *453*, 524–528.

Ye, L., Chang, Y.H., Xiong, Q., Zhang, P., Zhang, L., Somasundaram, P., Lepley, M., Swingen, C., Su, L., Wendel, J.S., et al. (2014). Cardiac repair in a porcine model of acute myocardial infarction with human induced pluripotent stem cell-derived cardiovascular cells. Cell Stem Cell *15*, 750–761.

Yusuf, F., Rehimi, R., Dai, F., and Brand-Saberi, B. (2005). Expression of chemokine receptor CXCR4 during chick embryo development. Anat. Embryol. (Berl) *210*, 35–41.

Zhang, X., Fang, H., Zhang, J., Yuan, Y., and Xu, W. (2011). Recent advance in aminopeptidase N (APN/CD13) inhibitor research. Curr. Med. Chem. *18*, 5011–5021.